Supporting Information

Nucleic Acid Functionalized Metal-Organic Frameworks-Based Homogeneous Electrochemical Biosensor for Simultaneous Detection of Multiple Tumor Biomarkers

Jiafu Chang,[a,b] Xin Wang,[a] Jiao Wang,[a] Haiyin Li,[a,*] and Feng Li[a,b,*]

[a] College of Chemistry and Pharmaceutical Sciences, Qingdao Agricultural University, Qingdao 266109, People's Republic of China

[b] College of Chemistry, Chemical Engineering and Materials Science, Shandong Normal University, Jinan 250014, People's Republic of China

* Corresponding author. Tel/Fax: 86-532-86080855;

E-mail: lifeng@qau.edu.cn

Table of Contents

EXPERIMENTAL SECTION

Chemical and Materials. All DNA and RNA were purchased from Shanghai Sangon Biotechnology Co. Ltd. (Shanghai, China) and TaKaRa Biotechnology Co., Ltd. (Dalian, China), respectively, with their sequences exhibited in Table S1. Zirconium oxide chloride octahydrate ($ZrOCl_2 \cdot 8H_2O$), 2-aminoterephthalic acid, 1-ethyl-3-(3-dimethylaminopropyl)carbodiimide (EDC), N-hydroxysulfosuccinimide (NHS), 3,3',5,5'-tetramethyl-benzidine (TMB), methylene blue (MB), CH_3COOH, Na_2HPO_4, NaH_2PO_4 and other reagents were ordered from Sigma-Aldrich (St. Louis, MO, USA) and used without further treatment.

Apparatus. X-ray diffraction (XRD) patterns were obtained using a Bruker D8 Advance X-ray diffractometer (Bruker, Germany). Transmission electron microscopy (TEM) images were recorded on an HT7700 microscope (Hitachi, Japan). X-ray photoelectron spectroscopy (XPS) was recorded on an ESCALAB 250Xi (Thermo Fisher S cientific, USA). Energy dispersive spectroscopy (EDS) mapping images and spectrum analysis we re conducted using a HITACHI S4800 SEM (Hitachi, Japan).Zeta potential measurement was recorded with a Nano Zetasizer ZS90 (Malvern, U.K.). Differential pulse voltammetric (DPV) measurements were carried out on an Autolab electrochemical workstation (Metrohm, Netherland) employing a three-electrochemical system. The fluorescence measurements were performed on an F-4600 fluorescence spectrometer (Hitachi, Japan). Fourier transform infrared spectra (FT-IR) were recorded using a NICOLET 380 FT-IR spectrometer (Nicolet Thermo, USA).

Table S1. Sequences of the oligonucleotides used in the experiments

Probe Name	Sequence (5′-3′)
C_{MB}	COOH-TGA GGT AGT AGG TT
P_{MB}	AA CTA TAC AA CCT ACT ACC TCA
let-7a	UGA GGU AGU AGG UUG UAU AGU U
let-7b	UGA GGU AGU AGG UUG UGU GGU U
let-7d	AGA GGU AGU AGG UUG CAU AGU U
C_{TMB}	COOH-TAG CTT ATC AGA CT
P_{TMB}	TG AAC ATC AG TCT GAT AAG CTA
miRNA-21	UAG CUU AUC AGA CUG AUG UUG A
miRNA-16	UAG CAG CAC GUA AAU AUU GGC G
miRNA-155	UUA AUG CUA AUC GUG AUA GGG GU

Table S2. miRNA assay performance of our strategy and other methods.

Method	Enzyme	Signal Molecule Labeling	Linear Range	Detection Limit	Ref.
Fluorescence	Yes	Yes	0.001~10000 pM	1 fM	1
Fluorescence	Yes	Yes	0.01~1000 pM	10 fM	2
Fluorescence	Yes	No	0.06~12.0 pM	10.8 fM	3
Chemiluminescence	Yes	No	0.01~50.0 pM	3.02 fM	4
Electroche-miluminescence	Yes	Yes	0.01~1000 fM	3.3 aM	5
Electrochemistry	No	Yes	0.005~500 pM	1.4 fM	6
Electrochemistry	Yes	Yes	0.01~5.0 fM	3.2 aM	7
Electrochemistry	Yes	No	0.01~1.0 pM	4.53 fM	8
electrochemistry	No	No	0.01~10.0 pM 0.02~10.0 pM	3.6 fM 8.2 fM	This work

Table S3. Recoveries and RSDs of the MOFs-based biosensor for let-7a and miRNA-21 spiked in human serum samples.

Sample No.	Added (pM)		Mean measured (pM)		Mean recovery [a] (%)		RSD (%)	
	let-7a	miRNA-21	let-7a	miRNA-21	let-7a	miRNA-21	let-7a	miRNA-21
1	0.1	0.1	0.0947	0.0963	94.7	96.3	4.75	4.07
2	1.0	1.0	1.0324	0.9736	103.0	97.4	3.89	3.20
3	3.0	3.0	3.1586	3.1267	105.0	104.0	4.16	4.38

[a]Recovery (%) = $100 \times (c_{\text{mean measured}} / c_{\text{added}})$

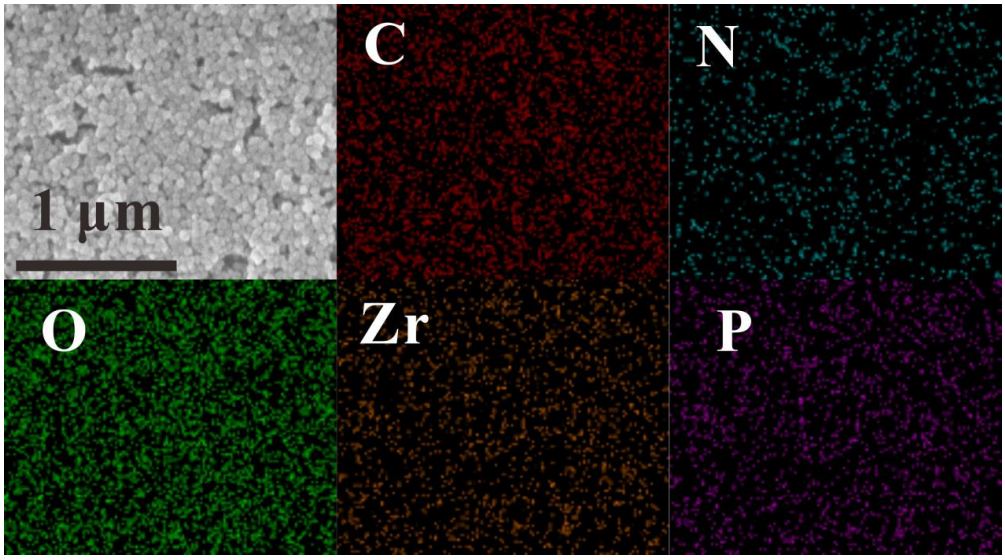

Figure S1. SEM and EDS mapping images of TMB@UIO and the corresponding distribution of C, N, O, Zr, and P elements.

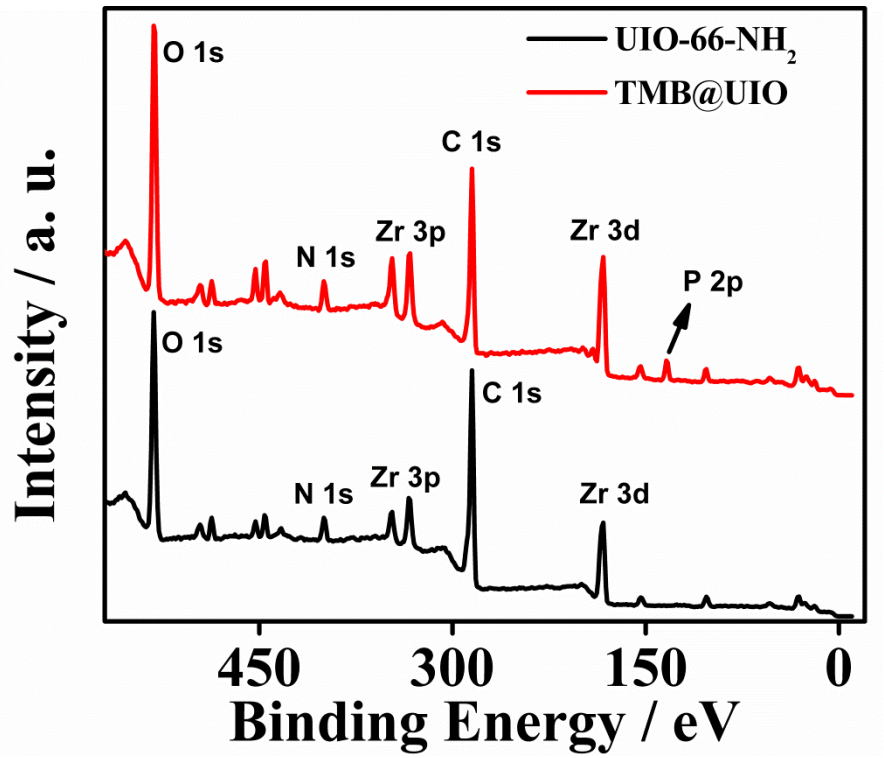

Figure S2. XPS curves of UIO-66-NH_2 and TMB@UIO.

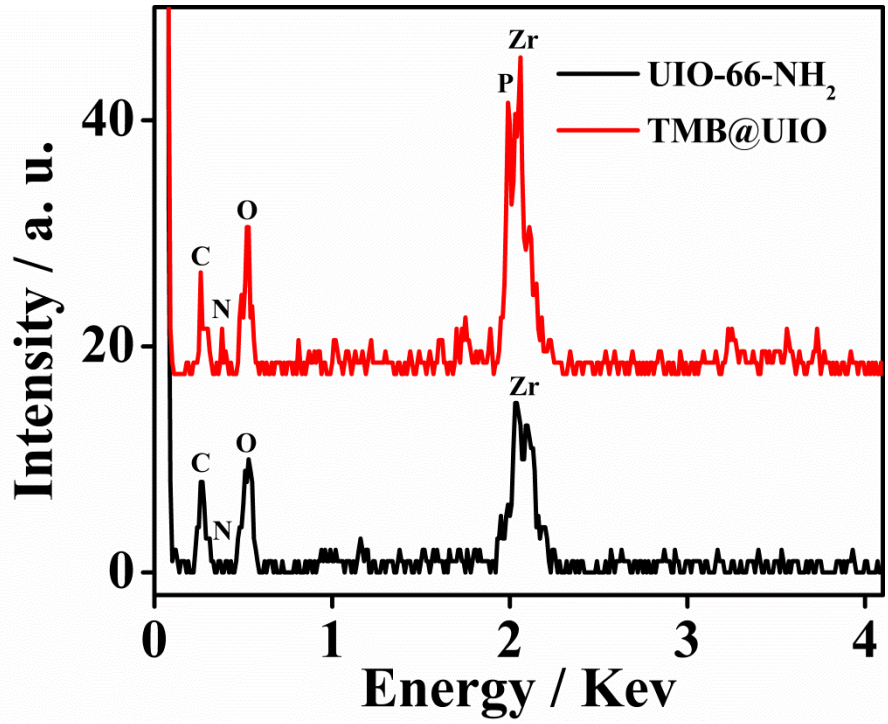

Figure S3. EDX spectra of UIO-66-NH_2 and TMB@UIO.

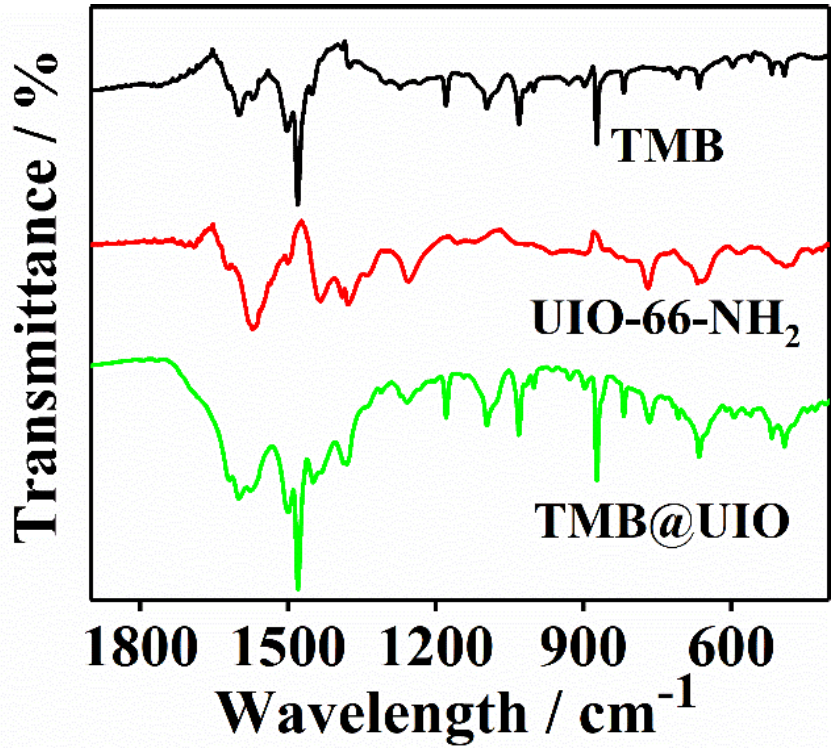

Figure S4. FT-IR spectra of TMB, UIO-66-NH_2, and TMB@UIO.

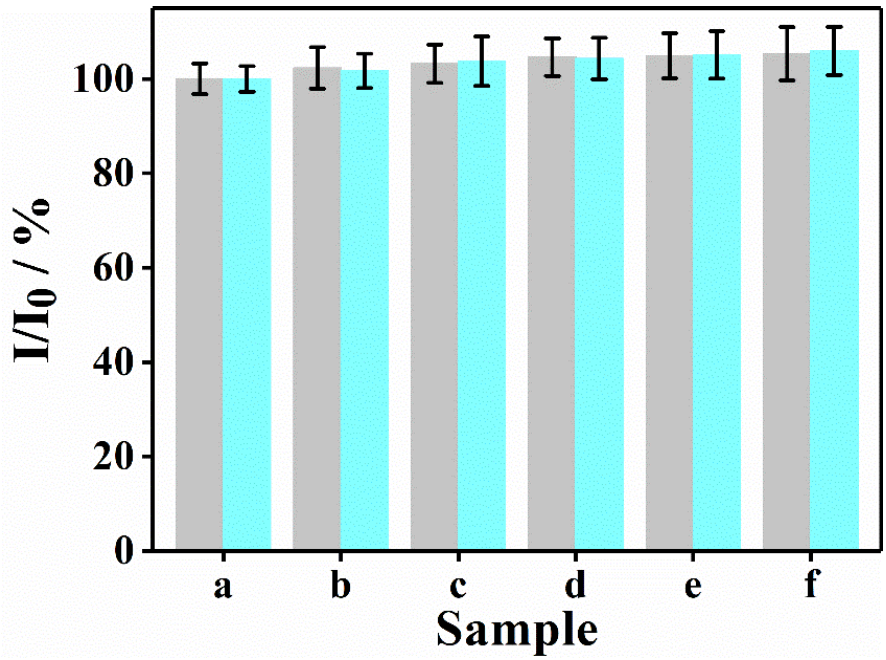

Figure S5. The stability of MB@UIO and TMB@UIO in PBS for different incubation times: a: 0 h, b: 1 h, c: 3 h, d: 5 h, e: 7 h, and f :in diluted human serum sample for 7 h.

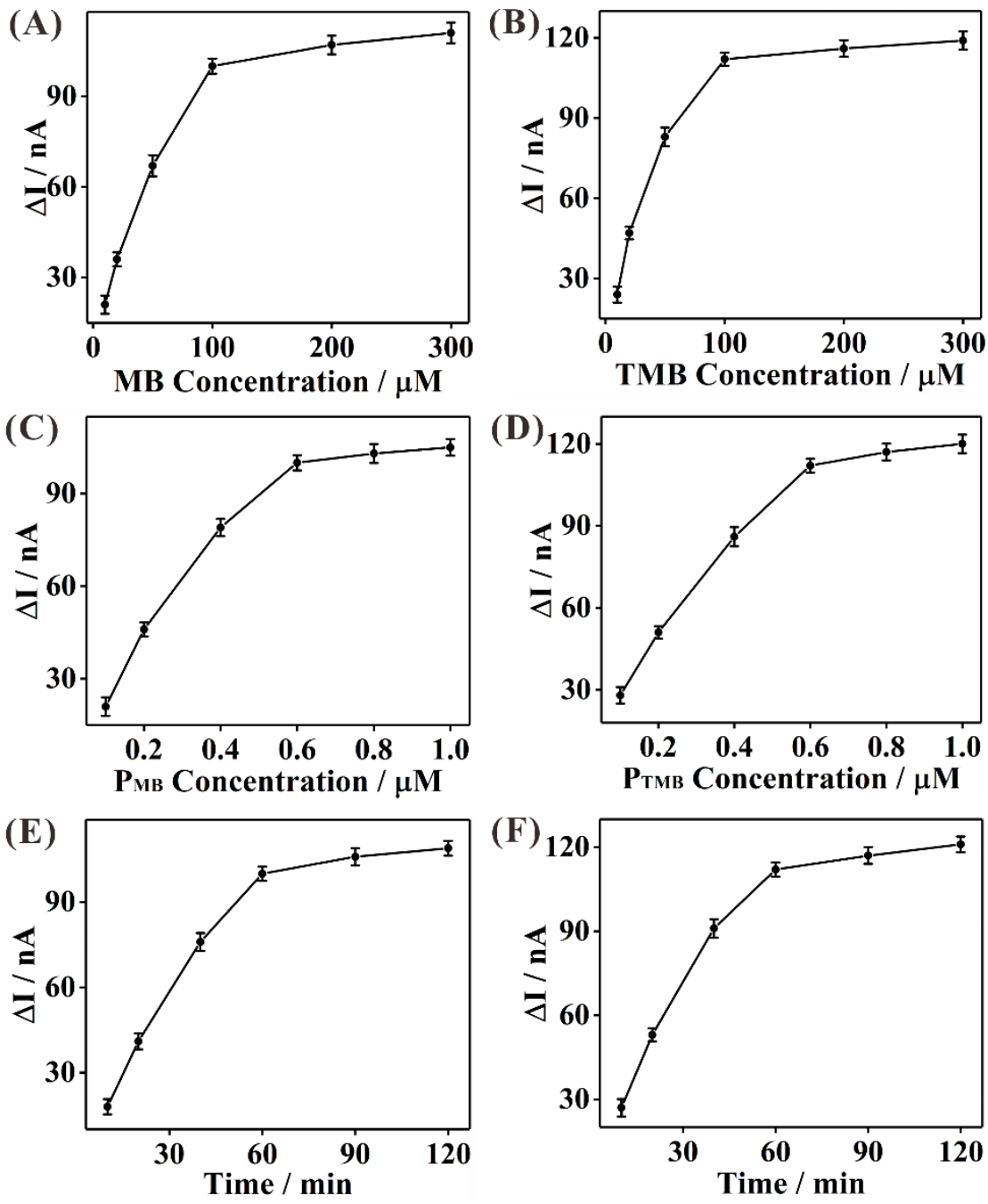

Figure S6. The DPV current changes (ΔI) of the proposed biosensor upon the addition of let-7a with different MB concentrations (A), P_{MB} concentrations (C), and the hybridization time between let-7a and MB@UIO (E). The DPV current changes (ΔI) of the proposed biosensor upon the addition of miRNA-21 with different TMB concentrations (B), P_{TMB} concentrations (D), and the hybridization time between miRNA-21 and TMB@UIO (F).

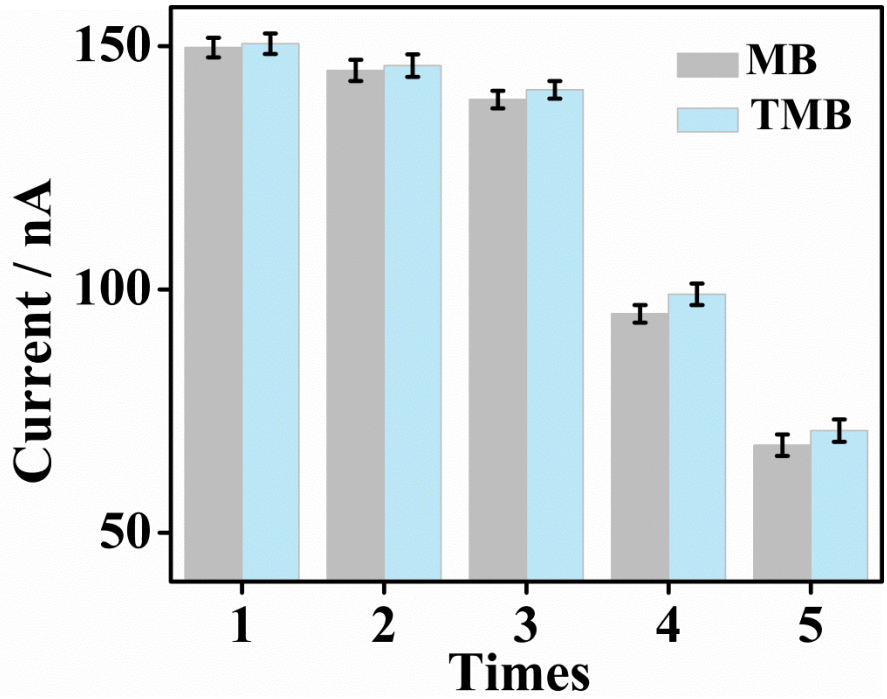

Figure S7. The reusability of C_x modified UIO-66-NH_2 in development of MB@UIO and TMB@UIO biosensors.

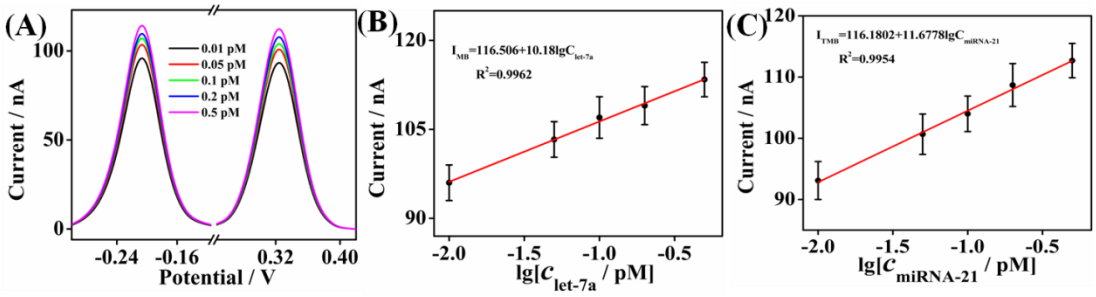

Figure S8. (A) The DPV curves of the proposed biosensor in the serum sample from breast cancer patient with different concentrations of let-7a and miRNA-21. (B) The linear relationship between the DPV current of MB and the logarithm of let-7a concentrations. (C) The linear relationship between the DPV current of TMB and the logarithm of miRNA-21 concentrations.

References

(1) Yin, B. C.; Liu, Y. Q.; Ye, B.-C., Sensitive Detection of MicroRNA in Complex Biological Samples via Enzymatic Signal Amplification Using DNA Polymerase Coupled with Nicking Endonuclease. *Anal. Chem.* **2013**, *85*, 11487–11493.

(2) Duan, R. X.; Zuo, X. L.; Wang, S. T.; Quan, X. Y.; Chen, D. L.; Chen, Z. F.; Jiang, L.; Fan, C. H.; Xia, F., Lab in a Tube: Ultrasensitive Detection of MicroRNAs at the Single-Cell Level and in Breast Cancer Patients Using Quadratic Isothermal Amplification. *J. Am. Chem. Soc.* **2013**, *135*, 4604–4607.

(3) Liu, H. Y.; Li, L.; Wang, Q.; Duan, L. L.; Tang, B., Graphene Fluorescence Switch-Based Cooperative Amplification: A Sensitive and Accurate Method to Detection MicroRNA. *Anal. Chem.* **2014**, *86*, 5487–5493.

(4) Ling, K.; Jiang, H.; Huang, X.; Li, Y.; Lin, J.; Li, F.-R., Direct Chemiluminescence Detection of Circulating MicroRNAs in Serum Samples Using a Single-strand Specific Nuclease-Distinguishing Nucleic Acid Hybrid System. *Chem. Commun.* **2018**, *54*, 1909–1912.

(5) Chen, A. Y.; Gui, G. F.; Zhuo, Y.; Chai, Y. Q.; Xiang, Y.; Yuan, R., Signal-off Electrochemiluminescence Biosensor Based on Phi29 DNA Polymerase Mediated Strand Displacement Amplification for MicroRNA Detection. *Anal. Chem.* **2015**, *87*, 6328–6334.

(6) Shi, K.; Dou, B. T.; Yang, C. Y.; Chai, Y. Q.; Yuan, R.; Xiang, Y., DNA-Fueled Molecular Machine Enables Enzyme-Free Target Recycling Amplification for Electronic Detection of MicroRNA from Cancer Cells with Highly Minimized Background Noise. *Anal. Chem.* **2015**, *87*, 8578–8583.

(7) Miao, P.; Jiang, Y.; Zhang, T.; Huang, Y.; Tang, Y., Electrochemical Sensing of Attomolar

MiRNA Combining Cascade Strand Displacement Polymerization and Reductant-Mediated Amplification. *Chem. Commun.* **2018**, *54*, 7366–7369.

(8) Shi, L.; Mu, C.; Gao, T.; Chen, T.; Hei, S.; Yang, J.; Li, G., DNA Nanoflower Blooms in Nanochannels: a New Strategy for MiRNA Detection. *Chem. Commun.* **2018**, *54*, 11391–11394.